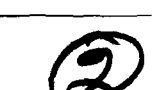

OFFICE OF NAVAL RESEARCH

Grant N00014-90-J-1971

R&T Code 4131pc1

Technical Report No. 9

High Resolution Infrared Spectroscopy of Formamide and Deuterated Formamide in a Molecular Beam

by

Christopher L. Brummel, Meihua Shen, Kevin B. Hewett, Laura A. Philips

Prepared for Publication
in the
Journal of the Optical Society of America, B

Cornell University
Department of Chemistry
Ithaca, NY 14853-1301

October 26, 1993

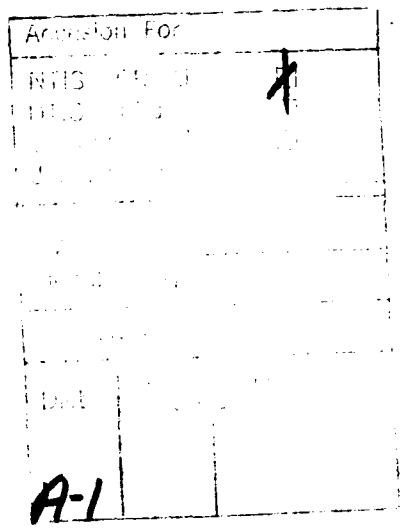

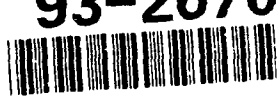

High resolution infrared spectroscopy of formamide and deuterated formamide in a molecular beam

Christopher L. Brummel, Meihua Shen, Kevin B. Hewett and Laura A. Philips.
Department of Chemistry, Cornell University, Ithaca, New York 14853.

Abstract

High resolution infrared spectra of formamide and deuterated formamide ($DCONH_2$) were collected using molecular beam optothermal spectroscopy. The spectrum of formamide was found to be perturbed such that each rotational transition was split into two peaks. The splitting was absent in the spectrum of deuterated formamide. The large splitting in the spectrum of formamide (~0.7 cm^{-1}) prevented an accurate deconvolution of the spectrum into zeroeth order bright and dark states. A list of the possible coupling modes is presented. The coupling, however, is not well represented as a simple coupling of two rigid rotors.

Introduction

Formamide is the simplest molecule containing a peptide link. Peptide links are the basis for assembling proteins and polypeptides from amino acids. The structure and flexibility of the peptide link determines the structure of proteins. Furthermore, a model for protein folding dynamics involves the flow of vibrational energy through the backbone structure of a protein.[1,2] Vibrational energy transfer from localized high frequency modes to the low frequency modes of the backbone structure are an important component such dynamics. Because of the biological relevance of formamide as a model of a peptide link, extensive experimental[3,4,5,6,7,8,9,10] and

theoretical[11,12,13,14,15,16,17,18,19,20,21] work has been performed to investigate both its structure and dynamics.

The structure of formamide has been the subject of some controversy. Two early microwave studies resulted in very different conclusions about the planarity of formamide. In one microwave study by Kurland and Wilson[10] a planar structure was proposed, but a separate microwave study by Costain and Dowling[4] on ten different isotopic species favored a non-planar structure. Later, in 1974, Hirota et. al.[6] determined a complete r_s structure of formamide from the microwave spectra of 14 isotopically substituted formamide species, and concluded formamide was planar. Several *ab initio* calculations were also performed to determine the potential energy surface and structure of formamide[11,12,13,14,15,16,17,18,19,20]. The results from the more recent experimental and theoretical studies, suggest that formamide has a very shallow single-minimum inversion potential near a planar structure[18,20,21]. Because of the shallow potential and the flexibility of the amino group, the molecule has a large non-zero effective inversion angle[18]. The shallow potential energy surface which allows the amino hydrogens to move out of the plane is the most probable source of many of the difficulties determining the structure of formamide.

The energy barriers for internal rotation about the C-N bond and the keto-enol tautomerization have also been the focus of study. A large barrier to internal rotation is expected because of the partial double bond character of the C-N bond. NMR studies in solution found a barrier to internal rotation of 18.5 kcal/mole[3]. The barrier to internal rotation in the gas phase is still unknown. The keto-enol tautomerization is of interest because it is a model of the keto-enol tautomerization in large heterocyclic systems, such as uracil, guanine and 2-pyridone systems. Unlike 2-pyridone, where the two

tautomers can thermally coexist, formamic acid is considerably less stable than formamide. While no experimental data is available, theoretical calculations predicted the energy difference between the two forms to be 12-13 kcal/mole and the activation energy barrier to be 49-60 kcal/mole[20].

In this paper, we present a high resolution infrared study of formamide in a molecular beam. We have investigated both formamide and deuterated formamide ($DCONH_2$). The rotationally resolved infrared spectrum provides information about the geometry of the molecule and about intramolecular dynamics occurring on the excited vibrational potential energy surface. By resolving individual eigenstates in the spectrum of formamide, the mechanism of vibrational mode coupling is also addressed. The goal of the present study is to explore both the structure and dynamics of formamide. Although some questions remain unanswered, the results presented here form a foundation for a better understanding of formamide.

Experimental

The formamide spectra reported in this paper were collected using an optothermal molecular beam spectrometer. The experimental apparatus has been described in detail elsewhere[22]. Briefly, the molecular beam was created by expanding a mixture of formamide and helium through a 50 μm nozzle. The resulting free jet was skimmed with a 500 μm skimmer located 2 1/2 cm from the nozzle. The liquid helium cooled bolometer (Infrared Laboratories Inc.) was placed 60 cm from the nozzle in the flight path of the molecular beam. The molecular beam was crossed with the infrared laser, in a multipassing configuration, 25 cm from the nozzle.

An F-center laser (Burleigh FCL-20) was used to produce high resolution infrared radiation. The F-center laser was pumped by an Argon

ion (Coherent, Innova 15) pumped dye laser (Coherent 599). The system produces 3-12 mW of tunable infrared radiation in the region of the symmetric N-H stretch of formamide at 3456-3428 cm^{-1}. To scan the F-center laser continuously, while remaining single-mode, a Macintosh II computer was used to control both the laser end mirror and the intracavity etalon synchronously. To monitor the high resolution scanning of the laser, two external confocal etalons were used, a scanning 7.5 GHz etalon and a fixed 750 MHz etalon. The scanning etalon was used, with a Wavelength Monitor (Digital Specialties) to produce a sawtooth wave with a period equal to the free spectral range of the etalon. The sawtooth voltage signal from the wavelength monitor was used to detect and correct for mode hops during the scans. The fixed etalon provided marker peaks 750 MHz apart which were later used to linearize the spectra. The etalon was calibrated daily with acetylene transitions of known frequency. The sensitivity of the instrument was also determined using these acetylene transitions. The signal-to-noise ratio for a typical acetylene scan is 30,000:1. The spectra were normalized for laser power fluctuations and bolometer desensitization. A portion of the raw data of the formamide spectrum with all the diagnostic traces is shown in Figure 1.

Formamide was purchased from Aldrich Chemical Company, and was used without further purification. Deuterated formamide was purchased from MSD Isotopes at a 99.3% purity and was also used without further purification. Formamide and the deuterated analog were seeded into the molecular beam by passing the helium carrier gas through a stainless steel reservoir which was located inside the vacuum chamber immediately behind the nozzle. The reservoir contained synthetic cotton which was saturated with the sample. To provide sufficient vapor pressure of the sample, both the

nozzle and the reservoir were heated. The nozzle was heated 5 °C higher than the reservoir to prevent condensation of the sample on the pinhole. Variations in the nozzle temperature and the backing pressure of the carrier gas were used to control the rotational temperature of the sample. Three spectra at different rotational temperatures were collected for formamide using the conditions shown in Table 1. The deuterated formamide spectra were collected with the nozzle temperature of 105/100 and an expansion pressure of 15 psig (2 atm).

Results and discussion

A high resolution infrared spectrum of formamide and deuterated formamide were collected with the molecular beam spectrometer described above. The spectra were taken in the 3456-3426 cm^{-1} region, which corresponds to the excitation of the symmetric NH stretching vibration in formamide.

Assigning quantum numbers to the spectrum of formamide was performed by calculating spectra and comparing them to the experimental spectrum. The ground state rotational constants of formamide were known from previous microwave studies[4,6,8]. As an initial guess the rotational constants for the ground state were used for both the excited state and the ground state when calculating spectra. Similarities between the calculated and experimental spectrum were then used to assign peaks in the experimental spectrum. To confirm the quantum number assignment, the ground state rotational constants were calculated by performing combination differences on the experimental spectrum. The peak spacing in the experimental spectrum was found to agree, to within experimental error, with the spacings predicted using the rotational constants determined from the microwave spectra. Peak intensity variations as a function of temperature

were used as a further check of quantum number assignments. Figure 2 shows stick spectra of formamide collected at the different temperatures.

After partial assignment of the spectrum, many peaks remained unassigned. The general features of the remaining peaks suggested the presence of a second vibrational band. The center of the second rotational envelope, is offset from the first vibrational envelope by 0.6730 cm^{-1} and has the same ground state rotational constants. Thus, the general features of the spectrum could be reproduced by two overlapping vibrational bands (Figure 3). The calculated spectra were calculated using a rigid rotor asymmetric top Hamiltonian with the same ground state rotational constants as determined by microwave spectroscopy. A list of assigned peaks and the deviations from the calculated fit are shown in Table 2a and Table 2b. All peaks of intensity 10% of the largest peak were assigned. The parameters which produced the best fit to the spectrum and the RMS deviation to the fit are shown in Table 3. Note that although the parameters in Table 3 produce a calculated spectrum which reproduces the general features of the experimental spectrum, the deviations to the fit are approximately 10 times larger than experimental error (0.0004 cm^{-1}).

The ground state rotational constants for formamide could be fit well using the same ground state rotational constants as the ones determined by microwave spectroscopy. The excited state rotational constants of the two different rotational envelopes could not be fit to within experimental error. Since there is only one fundamental vibration in the 3440 cm^{-1} region, the first question which must be addressed is the origin of what appears to be a second rotational envelope. The nearest fundamental vibration to the symmetric NH stretch is the asymmetric NH stretch, which is approximately 100 cm^{-1} higher in energy. Because of the large frequency separation between

the symmetric NH stretching vibration and all other fundamental vibrations we can be certain that the extra features in the spectrum are not due to the excitation of a different near degenerate fundamental vibration. Other combination bands would be predicted to have transitions in the spectral region of the NH stretch. The two rotational envelopes, however, have similar intensities, and the combination bands at similar frequencies would be expected to have significantly less intensity than the NH stretch fundamental.

There are several possible explanations for the extra features in the spectrum that can be ruled out because they are not consistent with the data. The different rotational envelopes cannot be due to the presence of clusters in the molecular beam because a cluster would not have the same ground state rotational constants as the formamide monomer. Similarly, the second rotational envelope cannot be due to an impurity in the sample since it is very unlikely an impurity would have the same ground state rotational constants as formamide. The possibility that one of the two bands is a vibrational hot band can be ruled out because the rotational constants for the first excited vibrational state of formamide are known from microwave spectroscopy and they do not agree with the ground state rotational constants of either rovibrational envelope. Also the intensity of a hot band is expected to change with temperature and no such intensity temperature dependence was found. Since the ground state of formamide has been well characterized by microwave spectroscopy[4,6,8], and our spectra are consistent with them, we conclude that the second band is due to some perturbation of the excited vibrational state.

The perturbations in the vibrational excited state could be due to tunneling splitting or mode coupling (Fermi, Coriolis, etc.). Tunneling

splitting at first appears to be a probable source of the perturbation since formamide contains an NH_2 group. The barrier height to the out of plane motion of the NH_2 hydrogens, however, is very small or nonexistent. If a barrier is present it is smaller than the zero point vibrational energy. Thus, the barrier is too small to produce the observed splittings. Another alternative barrier that could cause tunneling splitting is the internal rotation barrier about the C-N bond. This barrier to internal rotation (~18 kcal)[3], however, is too large to produce the observed splittings. Using a double well potential function with an 18.5 kcal barrier, the tunneling splitting is less than the experimental resolution until well above the frequency of the hydrogen stretching region. Thus, tunneling is not a likely source of the observed perturbations.

The other type of perturbation possible is vibrational mode coupling. Mode coupling has been observed in a variety of different experiments over the course of many years. More recently, high resolution infrared spectroscopy has revealed the presence of previously unobservable mode coupling in several different molecules. Some molecules that show such mode coupling in high resolution infrared spectra include 2-fluoroethanol[22], butyne,[23,24] ethanol[25], acetylene[26], and trifluoropropyne[27] . The nature of the mode coupling differs in the various molecules mentioned above, but in all cases the result is more peaks in the experimental spectrum than were expected from the rigid rotor/harmonic oscillator picture. The manifestation of mode coupling in formamide would be expected to be more restricted than the mode coupling in medium sized molecules like 2-fluoroethanol, butyne and trifluoropropyne because the density of potential coupling dark states is much lower in formamide. The density of states in formamide is calculated to be less than 1 state/cm^{-1}, while the density of states for the larger molecules

mentioned above is 40-100 state/cm^{-1} in the same spectral region. Thus, there are fewer states available to couple in formamide. The calculation of density of states in formamide was performed assuming that all of the vibrational modes, except for the two low frequency modes, were uncoupled oscillators with 1% anharmonicity, based on known fundamental frequencies from ref. 16. The remaining two low frequency modes are the C-N torsion and the N-H inversion. The C-N torsion energy levels were calculated explicitly assuming the double well potential described above. The N-H inversion energy levels were taken from ref. 6.

Mode coupling in the excited state can be used to explain the experimental spectrum of formamide. We know the perturbation is in the excited state and not the ground state since the microwave spectrum of the ground state can be fit using a rigid rotor[4] or, if greater precision is desired, a rigid rotor with centrifugal distortion constants[8]. The description of the formamide spectrum so far is consistent with the bright state coupling to a single dark state. If mode coupling splits each peak in the spectrum into two peaks, the resulting spectrum will appear to be two overlapping transitions as observed experimentally. Variation in the size of the coupling matrix element, as well as variations in the positions of the zeroeth order states, will generate variations in the spacings and intensities of these doublets, causing a departure from simple rigid rotor spectra

Several different coupling mechanisms could produce the splittings in the spectrum. Anharmonic, Coriolis, and centrifugal coupling are the most likely coupling mechanisms. Centrifugal coupling is not likely to be significant since we are examining only peaks with low quantum numbers. Generally centrifugal coupling is less significant for states of low quantum numbers, than for states of higher quantum numbers[28]. Furthermore,

inclusion of centrifugal distortion constants in the fitting procedure did not improve the fits sufficiently to warrant their inclusion. Neither Coriolis nor centrifugal coupling will split the J=0 energy level since the coupling matrix element for the J=0 level is zero in both cases. The spectrum of formamide shows the J=0 K_a=0 K_c=0 exited state energy level is split by approximately the same amount as other levels, therefore we conclude that the dominant mechanism must be anharmonic coupling.

If mode coupling is causing the perturbations in the spectrum the observed spectrum can be deconvolved to obtain the frequencies of the bright state and the perturbing dark state using the Lawrence/Knight[29] deconvolution procedure. The deconvolution would determine the size of the coupling matrix elements and would provide insight into the role of the different coupling mechanisms. Unfortunately the deconvolution procedure relies not only on the relative peak spacings, but also the relative peak intensities. Using intensity information in the deconvolution procedure is not a problem when the peaks with the same zeroeth order quantum number are closely spaced as is the case with 2-fluoroethanol and butyne. When the spectral splittings are large the errors in the intensity determination introduce large errors in the deconvolution. The frequency data is reproducible to 4 x 10^{-4} cm^{-1} but the intensity is only reproducible to 5% of full scale. Thus, if the two transitions are separated by ~0.7 cm^{-1}, our frequency information has approximately four decimal places, while our intensity information has two. Therefore the resulting deconvolved spectrum is limited by the intensity uncertainty. The size of the error introduced by the deconvolution procedure is greater than the deviations created by fitting the spectrum as two separate rotational envelopes.

Although we cannot accurately deconvolve the spectrum because of uncertainties in the intensity information, additional information can be extracted from the experimental data. For example, an upper limit on the magnitude of the coupling matrix element can be determined by assuming that the zeroeth order states are degenerate. In this scenario, the matrix element would be 0.35 cm^{-1}. Furthermore, we can determine whether the observed spectrum is produced by the coupling of two sets of rigid rotor energy levels, one corresponding to the fundamental vibration, the bright state and the other given by a combination band or overtone, the dark state. The test is performed by noting that the deconvolution is a change of basis set. A change of basis is the matrix transformation shown in equation 1.

$$\begin{bmatrix} E_L & H' \\ H' & E_D \end{bmatrix} \Leftrightarrow \begin{bmatrix} e_0 & 0 \\ 0 & e_1 \end{bmatrix} \qquad \text{eq 1}$$

Where e_0 and e_1 are the molecular eigenstates and E_L and E_D are the zeroeth order bright and dark states respectively. H' is the coupling matrix element which couples the bright and dark states. Since the trace of a matrix is invariant to transformations, the average positions of the molecular eigenstates will equal the average of the zeroeth order energy levels. If peaks from two rigid rotor spectra are averaged, the resulting average spectrum will be a rigid rotor spectrum[30]. Thus, assuming the experimental spectrum is produced by two coupled rigid rotor states, then it should be possible to average the frequencies of all the doublets in the spectrum and fit the average spectrum. If the spectrum is produced by two coupled rigid rotors, then the average spectrum should fit to a rigid rotor spectrum to within experimental error. The rotational constants obtained in this fashion would give little insight into the geometry of the vibrationally excited molecule, however the

deviations of the fit indicate whether the two coupled rigid rotors picture is consistent with the data. In formamide the fit to this average spectrum is not within experimental error (RMS dev.= 0.0028 cm^{-1}) thus, the formamide spectrum cannot be interpreted as simply two coupled zeroeth order rigid rotor sets of energy levels. There are two possibilities, either the zeroeth order energy levels are not those of a rigid rotor or more than two sets of energy levels are involved. It is possible that more than two sets of rigid rotor energy levels are interacting to produce the deviations in the spectrum, although the low density of states in this spectral region suggests that such an explanation would be a result of fortuitous accidental near resonances. The nonrigid rotor character of formamide could stem from the flexibility of the molecular structure. Flexibility of formamide would be somewhat surprising and could have important ramifications for the flexibility of the peptide links in protein structures.

Spectra of formamide deuterated by replacing the hydrogen on the carbon were also collected. The purpose of collecting a spectrum of deuterated formamide was to shift the position of the dark states in the molecule without affecting the fundamental nature of the vibration significantly.

Again the spectrum was fit by iteratively comparing calculated and experimental spectra. A qualitative good fit was achieved with a single rovibrational transition (Figure 4). Thus, the coupling which previously split each transition into two peaks was absent. The fit to the spectrum, however, was not within experimental error. The parameters which produced the best fit are shown in Table 4 and a list of all of the assigned peaks is given in Table 5. Inclusion of centrifugal distortion constants, again did not bring the fit in agreement with experiment. The center frequency for the fit is almost unaffected by the deuteration on the nitrogen, indicating that the

fundamental vibration is only slightly affected by the deuteration as predicted. The center frequency for the N-H stretch in deuterated formamide was measured to be shifted 1.05 cm^{-1} with respect to the rotational envelope with greater intensity in the undeuterated species, and 0.69 cm^{-1} with respect to the average of the frequencies of the of the two bands.

The additional data from deuterated formamide demonstrates that there are at least two factors at play in producing the deviations from a rigid rotor in formamide. First, there is mode coupling which splits each transition into two transitions separated by approximately 0.7 cm^{-1} and second, there is a perturbation which causes the spectrum to deviate from that of a rigid rotor. The elimination of the splittings in the spectrum supports the conclusion that tunneling is not the source of the splitting, because replacing the hydrogen on the carbon with a deuterium would not significantly affect the tunneling of the hydrogens on the nitrogen.

Elimination of the splitting upon deuteration also indicates that we have sufficiently shifted the position of the coupling dark state so that it no longer couples to the bright state. This difference between deuterated and undeuterated formamide provides some information as to the identity of the coupling dark state. We know that the vibration must contain some motion of the hydrogen on the carbon, but only small motions of the hydrogen (or deuterium) are necessary to move the position of the dark state. Thus, only a few modes are eliminated as possible candidates for the dark state. The coupling state must also be of A' symmetry of the C_S point group. Finally, identification of the coupling dark state hinges on an accurate knowledge of the fundamental vibrations of both formamide and its deuterated analog. Unfortunately, these values are not known very accurately. Thus, when determining all possible candidates for coupling one must allow for

substantial error. Because of these limitations, we cannot uniquely identify a single mode as the coupling mode but Table 6 lists the seven possible candidates within 10 cm^{-1} of the observed transition frequency, and Table 7 contains the fundamental frequencies used in the analysis.

Included in Table 6 are a wide range of vibrational modes. These different vibrational modes generate substantially different motions within the molecule, and therefore different equilibrium geometries. Since each of these geometries would give rise to different excited state rotational constants, comparison of the possible rotational constants with the experimentally determined rotational constants provides further information regarding the identity of the dark state. Calculated estimations of the excited state rotational constants will, of course, be approximations, but even crude approximations argue strongly against some of the vibrational modes in Table 6. The geometry of the excited N-H stretch alone is not sufficient to account for the difference between the ground and excited state rotational constants, consistent with vibrational mode-coupling. Furthermore, consistent with the results of the study of deuterated formamide, some bending motion of the C-H bond is required, either in plane or out of plane. Finally, examination of the change in the inertial defect provides additional information regarding the geometry of the dark state. In the ground state, the inertial defect is small and positive[6], $\Delta = 0.0082$ μÅ. From the two sets of excited state rotational constants determined in the present study, a negative inertial defect is found, $\Delta = -0.069$ μÅ and -0.086 μÅ. A negative inertial defect is suggestive of an out of plane motion.[31] These considerations limit the possible modes to the first 4 modes listed in Table 6. These 4 modes contain from 5 to 8 quanta of vibrational excitation. The most probable coupling mode would be the modes of least quanta

Conclusions

We have collected and assigned spectra of formamide and deuterated formamide in the symmetric NH stretching region. Combination differences in the ground state reproduce the expected peak spacings based on the rotational constants determined from microwave spectroscopy for both molecules. The spectrum of formamide indicates that the NH stretch is coupled to another vibrational mode causing the peaks in the spectrum to be split into doublets. The dominant mechanism of the coupling is anharmonic coupling, although other coupling mechanisms are present to a lesser extent. In the spectrum of deuterated formamide, there was no evidence of doublets. The deuterated formamide spectrum is evidence that mode coupling in formamide involves some motion of the CH group. A list of possible coupling modes is shown in Table 6. The presence of mode coupling implies that the vibrational motion excited in the NH stretching region is not accurately depicted as the symmetric NH stretching normal mode. The motion is rather, a more complicated superposition of several normal modes, and excitation of the "NH stretch" effectively deposits energy in other lower frequency modes of the molecule.

Acknowledgments: This work is supported by: The National Institute of Health under grant #08-R9N527039A, The Office of Naval Research under grant #N00014-90-J-1971, The Petroleum Research Fund administered by the American Chemical Society. The authors are grateful to the referees for several helpful suggestions.

References:

(1) M. M. Teeter; D. A. Case, "Harmonic and Quasiharmonic Descriptions of Crambin",J. Phys. Chem. 94, 8091 (1990).

(2) M. Levitt; C. Sander; P. S. Stern, "Protein Normal-Mode Dynamics: Trypsin Inhibitor, Crambin, Ribonuclease and Lysozyme",J. Mol. Biol. 181, 423 (1985).

(3) T. Drakenberg; S. Forsen, "The Barrier to Internal Rotation in Amines. I. Formamide",J. Phys. Chem. 74, 1 (1970).

(4) C. C. Costain; J. M. Dowling, "Microwave Spectrum and Molecular Structure of Formamide",J. Chem. Phys. 32, 158 (1953).

(5) J. C. Evans, "Infrared Spectrum and Thermodynamic functions of Formamide",J. Chem. Phys. 22, 1228 (1953).

(6) E. Hircta; R. Sugisaki; J. C. Nielsen; G. O. Sørensen, "Molecular Structure and Internal Motion in Formamide from Microwave Spectrum",J. Mol. Spectrosc. 49, 251 (1974).

(7) S. T. King, "Infrared Study of the NH_2 "Inversion" Vibration of Formamide",J. Phys. Chem. 75, 405 (1971).

(8) W. H. Kirchhoff; D. R. Johnson, "An Investigation of Centrifugal Distortion in the Microwave Spectrum of Formamide",J. Mol. Spectrosc. 45, 159 (1973).

(9) Y. Sugawara; Y. Hamada; M. Tsuboi, "Vibration-rotation Spectra of Formamide",Bull. Chem. Soc. Jpn. 56, 1045 (1983).

(10) R. J. Kurland; E. B. Wilson, "Microwave spectrum structure, dipole moment and quadrupole coupling constants of formamide.",J. Chem. Phys. 27, 585 (1957).

(11) N. R. Carlsen; L. Radom; N. V. Riggs; W. R. Rodwell, "Is Formamide Planar of Nonplanar?",J. Am. Chem. Soc. 101, 2233 (1979).

(12) Y. Sugawara; Y. Hamada; A. Y. Hirakawa; M. Tsuboi; S. Kato; K. Morokuma, "Ab Initio MO Calculation of Force Constants and Dipole Derivatives for Formamide",J. Chem. Phys. 50, 105 (1980).

(13) C. W. Bock; M. Trachtman, P. George, "A Comparative Ab Initio Study of the Structures, Dipole Moments, Force Fields, and Anharmonic Frequencies of Formamide and Thioformamide",J. Mol. Spectrosc. 89, 76 (1981).

(14) T. J. Zielinski; R. A. Poirier; M. R. Peterson; I. G. Csizmadia, "Conformational Study of Protonated Formamide",J. Comput. Chem. 3, 477 (1982).

(15) H. B. Schlegel; P. Grund; E. M. Flunder, "Tautomerization of Formamide, 2-Pyridone, and 4-Pyridone: An Ab Initio Study",J. Am. Chem. Soc. 104, 5247 (1982).

(16) G. Fogarasi; A. Balázs, "A Comparative Ab Initio Study of Amides. Part I. Force Fields and Vibrational Assignments for formamide, acetamide and N-methylformamide",J. Mol. Struct. 133, 105 (1985).

(17) P. G. Jasien; W. J. Stevens; M. Krauss, "Ab Initio Calculations on the Rotational Barriers in Formamide and Acetamide: The Effects of Polarization Functions and Correlation",J. Mol. Struct. 139, 197 (1986).

(18) R. D. Brown; P. D. Godfrey; B. Kleibömer, "The Conformation of Formamide",J. Mol. Spectrosc. 124, 34 (1987).

(19) J.-H. Lii; N. L. Allinger, "The MM3 Force Field for Amides, Polypeptides and Proteins",J. Comp. Chem. 12, 186 (1991).

(20) X.-C. Wang; J. Nichols; M. Feyereisen; M. Gutowski; J. Boatz; A. D. J. Haymet; J. Simons, "Ab Initio Quantum Chemistry of Formamide-Formamidic Acid Tautomerization",J. Phys. Chem. 95, 10419 (1991).

(21) K. B. Widberg; C. M. Breneman, "Resonance interactions in acyclic systems. 3. Formamide internal rotation revisited. Charge and energy redistribution along the C-N bond rotation pathway.",J. Am. Chem. Soc. 114, 831 (1992).

(22) C. L. Brummel; S. W. Mork; L. A. Philips, "High-resolution Infrared Spectroscopy of 2-Fluroethanol in a Molecular Beam",J. Chem. Phys. 95, 7041 (1991).

(23) A. M. de Souza; D. Kaur; D. S. Perry, "Vibrational State Mixing of Individual Rotational Levels in 1-Butyne near 3333 cm^{-1}",J. Chem. Phys. 88, 4569 (1988).

(24) A. Mcllroy; D. J. Nesbitt, "Vibrationa Mode Mixing in Terminal Acetylenes: High-Resolution Infrared Laser Study of Isolated *J* States",J. Chem Phys. 92, 2229 (1990).

(25) J. Go; G. A. Bethardy; D. S. Perry, "Rotationally Mediated Intramolecular Vibrational Redistribution in Jet-Cooled *trans*-Ethanol at 2990 cm^{-1}",J. Phys. Chem. 94, 6153 (1990).

(26) W. J. Lafferty; R. J. Thibault, "High resolution infrared spectra of C_2H_2, C12C13H2, and $(C13)_2H_2$",J. Mol. Spectrosc. 14, 79 (1964).

(27) B. H. Pate; K. K. Lehmann; G. Scoles, "The onset of intramolecular vibrational energy redistribution and its intermediate case: The v1 and 2v1 molecular beam, optothermal spectra of trifluoropropyne.",J. Chem. Phys. 95, 3891 (1991).

(28) A. E. W. Knight, "Rotational involvement in intramolecular vibrational redistribution."; In: Excited States. Ed. by E. C. Lim and K. K. Innes. (Academic Press: San Diego, 1988) 1.

(29) W. D. Lawrence; A. E. W. Knight, "Direct deconvolution of extensively perturbed spectra: The singlet-triplet molecular eigenstate spectrum of pyrazine",J. Phys. Chem. 89, 917 (1985).

(30) If two rigid rotor spectra are averaged peak for peak the resulting new spectrum will be well characterized by a rigid rotor. If the difference in the rotational constants of the two original spectra is small the rotational constants for the average spectrum will be the average of the rotational constants of the original spectra.

(31) Y. M. Takeshi Oka, "Calculation of Inertia Defect",J. Mol. Spectrosc. 6, 472 (1961).

Figure Captions

Figure 1: The figure shows the data collected during a typical scan. Trace A is the output of a fixed marker etalon. The irregularities in the baseline are artifacts that result from baseline subtraction. Trace B is the output of a scanning etalon after being processed by the wavelength monitor. Trace C is the output of the laser power meter and trace D is the output of the lock-in amplified bolometer detector. The high frequency peak is assigned to be a doublet and all other features are individual peaks. All individual peaks have the same FWHM within experimental uncertainties.

Figure 2: The figure shows three spectra of formamide collected at different temperatures. These spectra are a plot of the position and intensities of the peaks as determined from the raw data (see text). The rotational temperature was controlled by changing the expansion conditions of the molecular beam.

Figure 3: The figure shows the experimental spectrum (A) and the best fit to the experimental spectrum using the superposition of two calculated rotational envelopes (B). Panels C and D show the two different calculated spectra separately.

Figure 4: The figure shows the experimental spectrum of deuterated formamide (A) and the best calculated fit to the data (B).

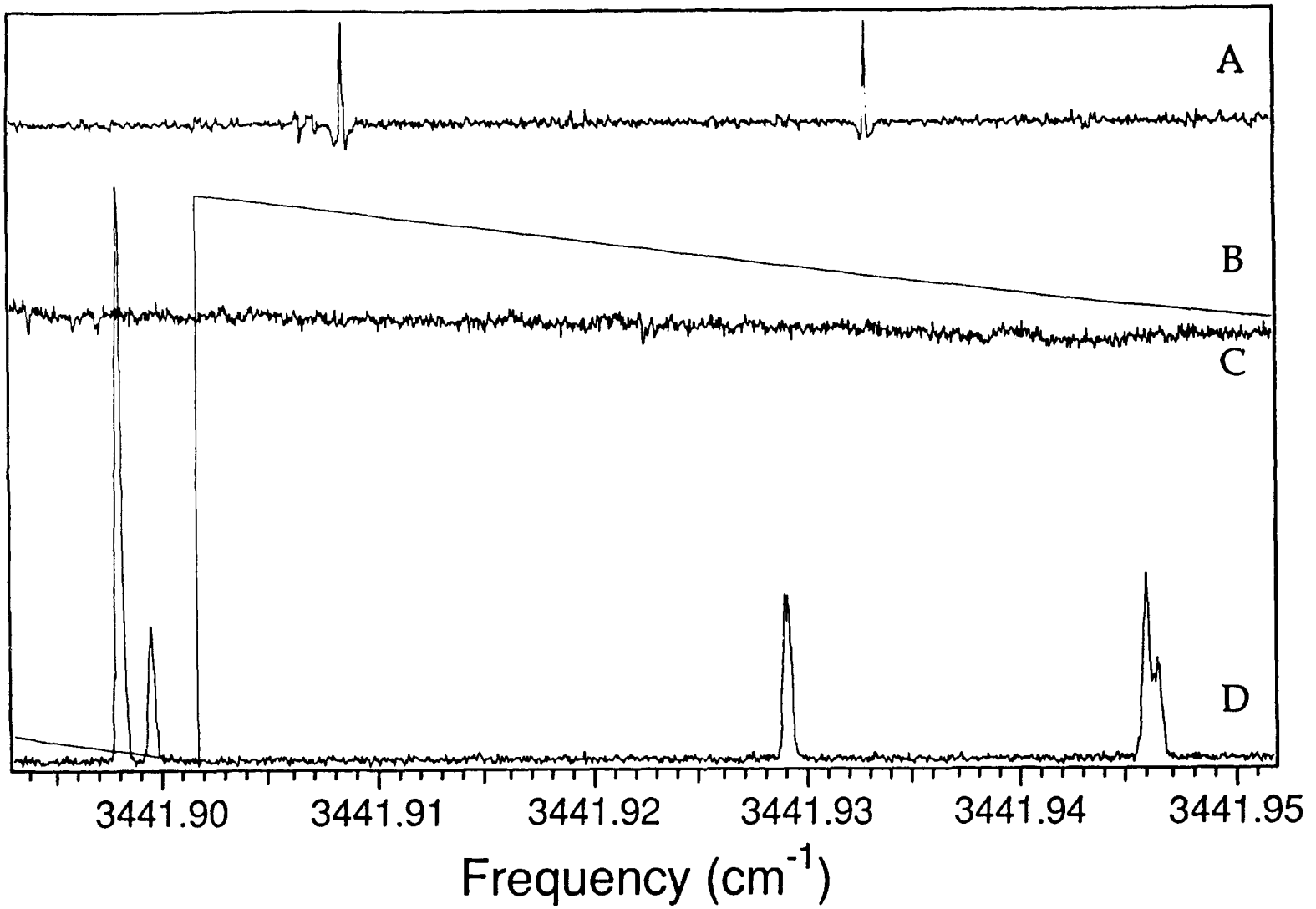
A
B
C
D
3441.90
3441.91
3441.92
3441.93
3441.94
3441.95
Frequency (cm-1)

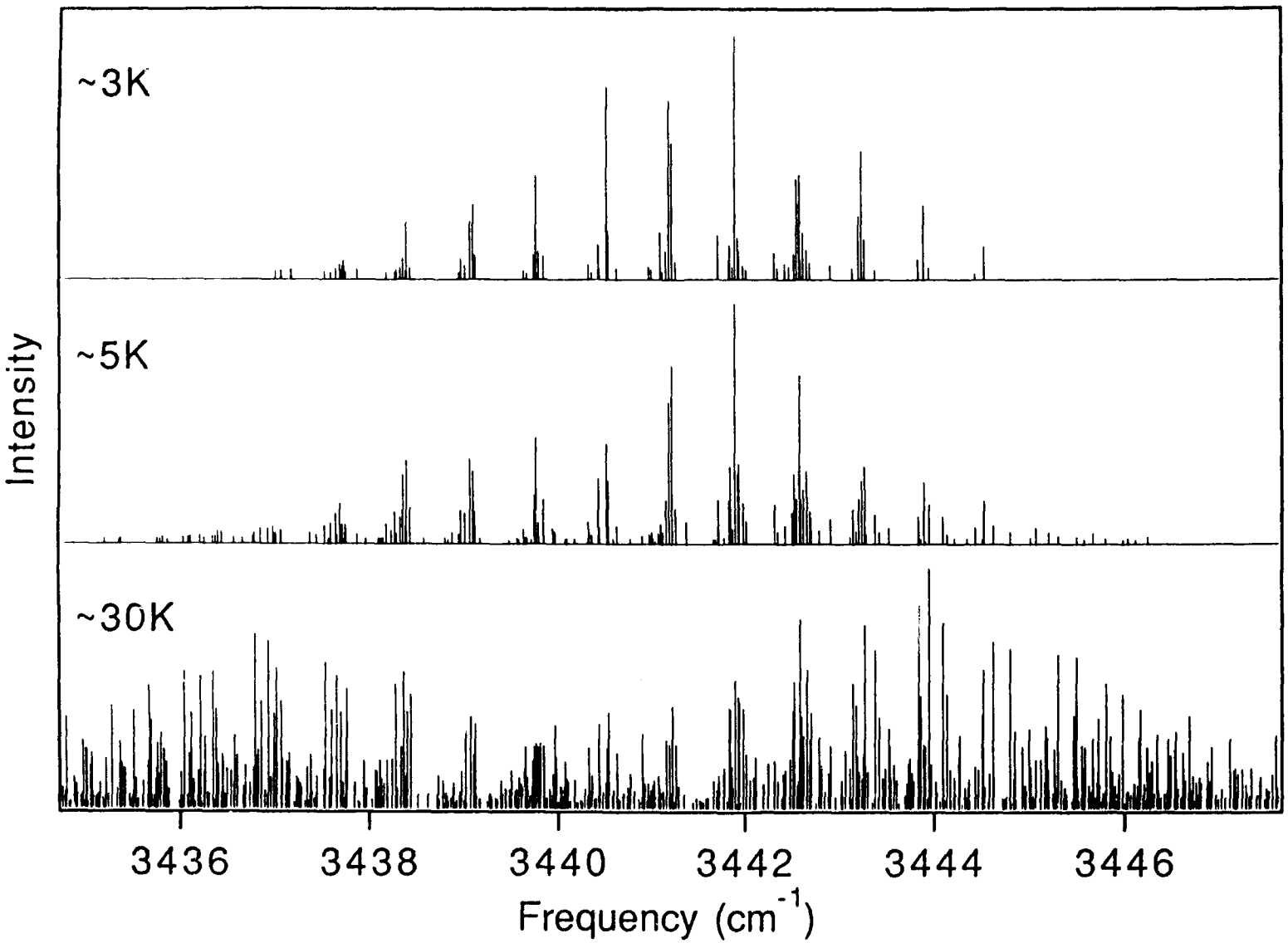
~3K
~5K
~30K
Intensity
3436
3438
3440
3442
3444
3446
Frequency (cm-1)

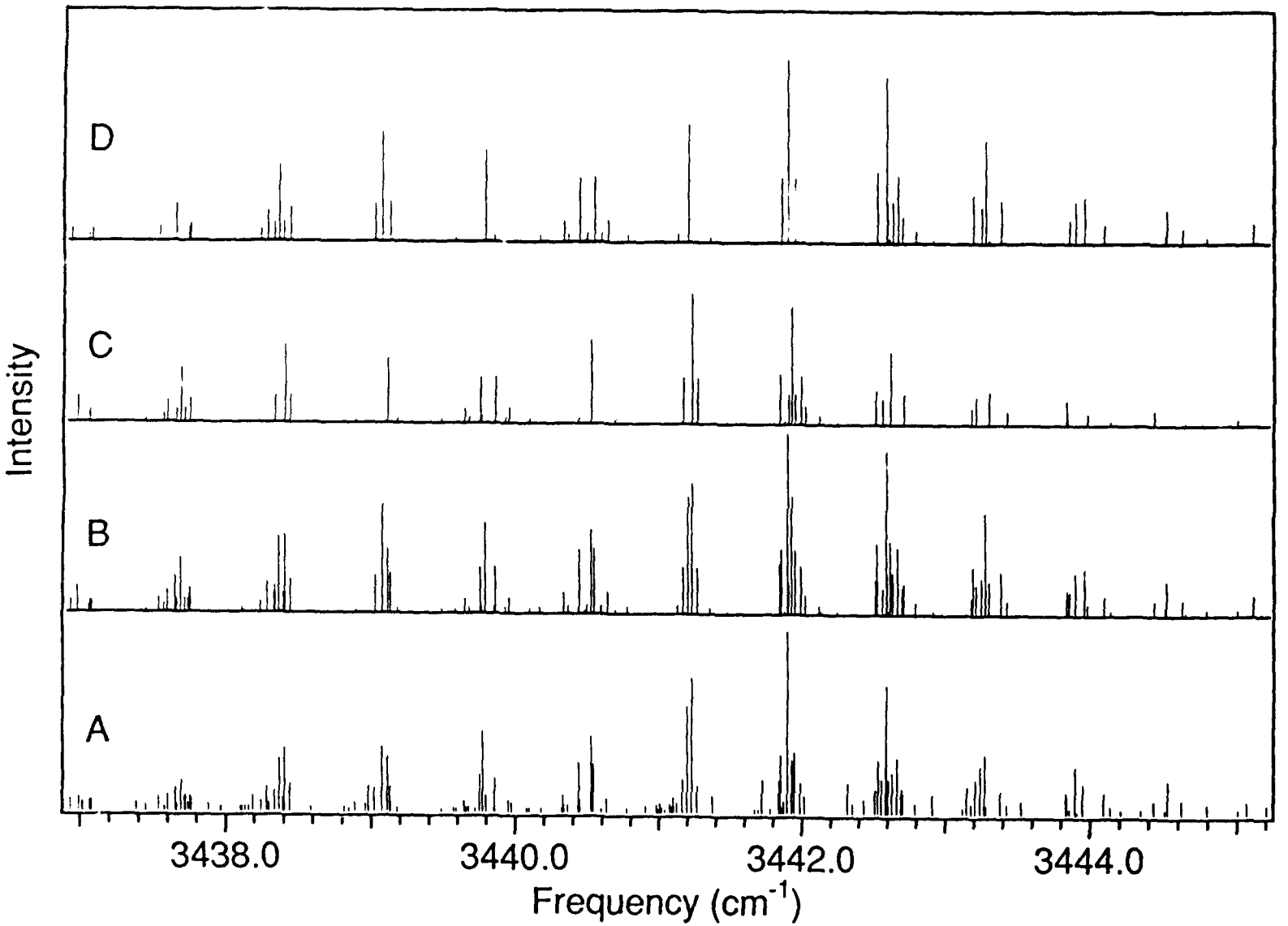
D
C
B
A
Intensity
3438.0
3440.0
3442.0
3444.0
Frequency (cm-1)

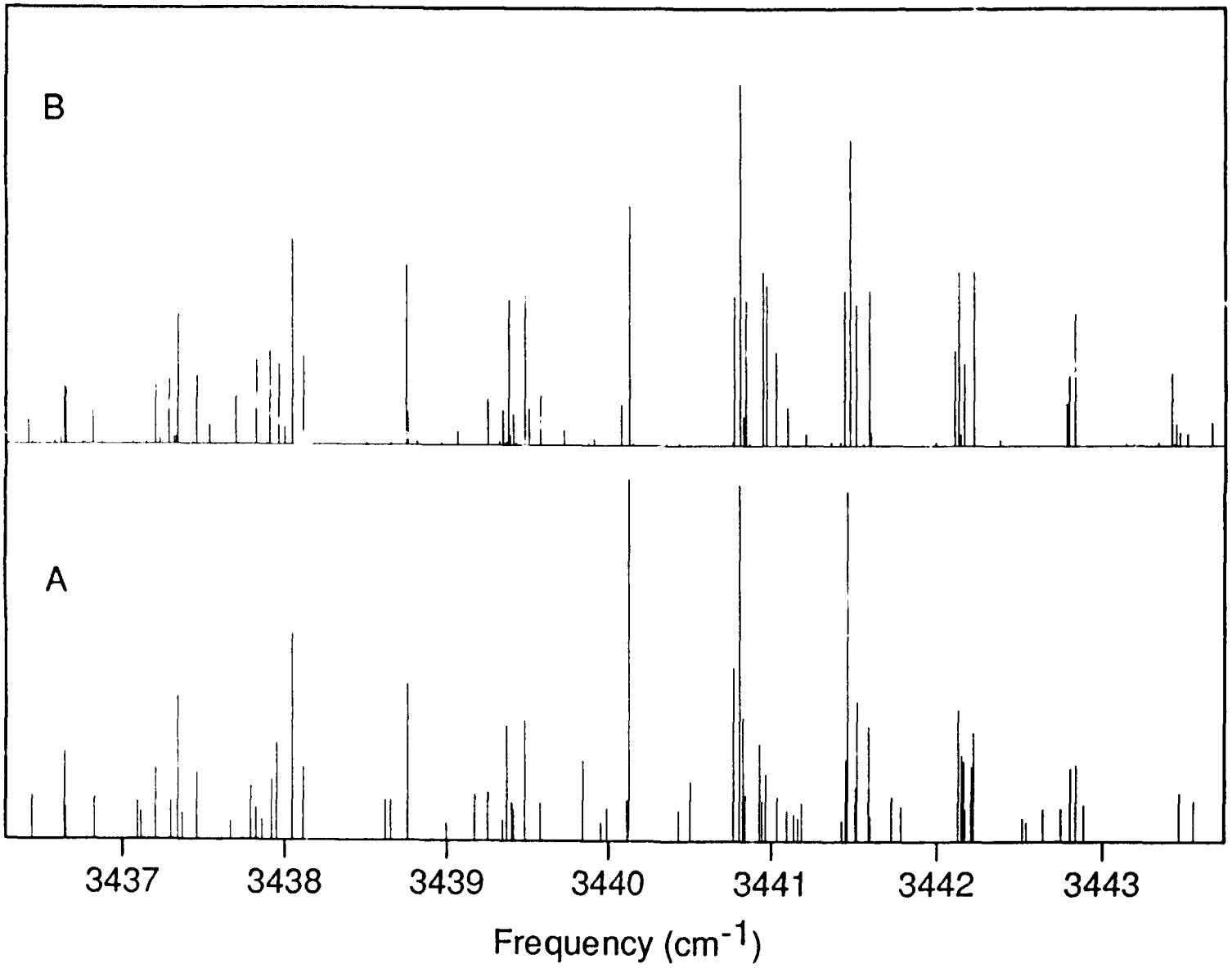
B
A
3437
3438
3439
3440
3441
3442
3443
Frequency (cm-1)

Table 1: Experimental conditions		
Helium Backing Pressure (atm /psig)	Temperature of Nozzle (K)	Rotational Temperature (K)
1.3 /4	122	30
4.4 /50	100	6
6.8 /100	83	4

Table 2a: Assignments for peaks in spectrum I and deviations from the best fit. Values in cm^{-1}.

J'	K_a'	K_c'	J"	$K_a"$	$K_c"$	Observed	Δ
6	0	6	5	0	5	3444.6232	-0.0013
3	1	3	2	0	2	3444.5268	0.0121
6	1	6	5	1	5	3444.5091	0.0008
5	1	4	4	1	3	3444.0923	0.0032
5	0	5	4	0	4	3443.9474	-0.0055
2	1	2	1	0	1	3443.8950	0.0011
5	1	5	4	1	4	3443.8391	-0.0103
4	1	3	3	1	2	3443.3803	0.0000
4	0	4	3	0	3	3443.2722	-0.0013
1	1	1	0	0	0	3443.2426	-0.0018
3	1	2	3	0	3	3442.6966	-0.0011
3	1	2	2	1	1	3442.6648	-0.0014
2	1	1	2	0	2	3442.6285	-0.0022
3	0	3	2	0	2	3442.5902	0.0033
1	1	0	1	0	1	3442.5853	-0.0020
2	1	1	1	1	0	3441.9455	-0.0015
2	0	2	1	0	1	3441.8977	0.0039
1	0	1	0	0	0	3441.1942	-0.0009
1	1	1	2	0	2	3441.1215	-0.0017
2	1	1	2	1	2	3440.6329	-0.0020
1	1	0	1	1	1	3440.5389	-0.0022
1	1	1	1	1	0	3440.4384	-0.0011
2	1	2	2	1	1	3440.3318	0.0017
0	0	0	1	0	1	3439.7697	-0.0144
1	1	1	2	1	2	3439.1261	-0.0013
1	0	1	2	0	2	3439.0730	-0.0008
1	1	0	2	1	1	3439.0218	-0.0018
2	1	2	3	1	3	3438.4405	0.0009
1	0	1	1	1	0	3438.3896	-0.0005
2	0	2	3	0	3	3438.3662	0.0047
2	0	2	2	1	1	3438.3347	0.0046
2	1	1	3	1	2	3438.2807	-0.0015
3	0	3	3	1	2	3438.2423	0.0039
3	1	3	4	1	4	3437.7626	0.0133
3	0	3	4	0	4	3437.6526	0.0042
3	1	2	4	1	3	3437.5365	-0.0007

Table 2b: Assignments for peaks in spectrum II and deviations from the best fit. Values in cm^{-1}.

J'	K_a'	K_c'	J''	K_a''	K_c''	Observed	Δ
3	1	3	2	0	2	3443.8327	0.0003
2	1	2	1	0	1	3443.2075	-0.0010
4	1	3	3	1	2	3442.7072	0.0014
4	0	4	3	0	3	3442.6025	-0.0099
4	1	4	3	1	3	3442.5095	0.0016
3	1	2	3	0	3	3442.0176	0.0001
3	1	2	2	1	1	3441.9862	0.0001
3	0	3	2	0	2	3441.9290	0.0079
1	1	0	1	0	1	3441.8992	-0.0009
3	1	3	2	1	2	3441.8376	0.0010
2	1	1	1	1	0	3441.2624	-0.0003
2	0	2	1	0	1	3441.2264	0.0019
2	1	2	1	1	1	3441.1618	-0.0004
1	0	1	0	0	0	3440.5229	-0.0004
2	1	1	2	1	2	3439.9501	-0.0005
1	1	0	1	1	1	3439.8531	-0.0009
1	1	1	1	1	0	3439.7514	-0.0006
2	1	2	2	1	1	3439.6443	-0.0005
0	0	0	1	0	1	3439.1100	-0.0011
1	1	1	2	1	2	3438.4387	-0.0013
1	0	1	2	0	2	3438.4019	-0.0002
1	1	0	2	1	1	3438.3362	-0.0003
2	1	2	3	1	3	3437.7537	-0.0005
2	0	2	3	0	3	3437.6940	0.0017
2	1	1	3	1	2	3437.5981	0.0002
3	1	3	4	1	4	3437.0687	0.0017
3	1	2	4	1	3	3436.8581	0.0010

Table 3: Rotational constants for formamide. The ground state constants are taken from reference 4. The excited state rotational constants are those obtained by treating the spectrum as two overlapping transitions. All values in cm^{-1}.

	Ground State	Spectrum I	Spectrum II
A	2.425575	2.4262 (18)	2.4113 (12)
B	0.3793943	0.37689 (19)	0.37767 (16)
C	0.3280255	0.32665 (14)	0.32707 (16)
RMS dev		0.0048	0.0026
Δ Center Frequency = 0.6729(15)			

Table 4: Rotational constants for the deuterated formamide. The ground state values are taken from reference 4. All values in cm^{-1}.

	Ground State	Excited State
A	1.832858	1.8234 (22)
B	0.3793601	0.36627 (46)
C	0.314204	0.32166 (46)
RMS dev.		0.0048

Table 5: Quantum number assignment for deuterated formamide and the deviations to the fit for a total of 23 peaks, RMS dev= 0.005813

J'	K_a'	K_c'	J"	K_a''	K_c''	Observed	Δ
0	0	0	1	0	1	3438.7547	0.0083
1	0	1	0	0	0	3440.1297	0.0040
1	0	1	2	0	2	3438.0517	0.0046
1	1	0	1	0	1	3440.9314	-0.0074
1	1	0	1	1	1	3439.4782	-0.0070
1	1	1	1	1	0	3439.3737	-0.0026
1	1	1	2	1	2	3438.1174	-0.0021
2	0	2	1	0	1	3440.8010	-0.0015
2	0	2	3	0	3	3437.3440	-0.0013
2	1	1	2	0	2	3440.9676	-0.0013
2	1	1	1	1	0	3440.8341	-0.0012
2	1	1	2	1	2	3439.5777	-0.0008
2	1	1	3	1	2	3437.2055	-0.0004
2	1	2	1	0	1	3442.2205	-0.0023
2	1	2	1	1	1	3440.7673	-0.0020
2	1	2	2	1	1	3439.2504	-0.0014
2	1	2	3	1	3	3437.4637	-0.0019
3	0	3	2	0	2	3441.4666	-0.0043
3	1	2	3	0	3	3441.0356	0.0165
3	1	3	2	1	2	3441.4459	0.0075
3	1	3	4	1	4	3436.8256	0.0086
4	0	4	3	0	3	3442.1222	-0.0099
4	1	3	4	0	4	3441.0927	-0.0017

Table 6: Possible coupling modes. Each normal mode is enclosed in parenthesis. The list of atoms inside the parenthesis describe the vibration. The number before the parenthesis indicates the number of quanta in that normal mode. All possible modes are included, but the most probable modes, based on geometry arguments are the first five modes. The notation refers to various vibrational modes as follows:

ν = stretch, ∂ = bend, r = rock, τ = torsion, w = out of plane wag.

3434.23 cm^{-1}	1(wCH) + 2(∂NCO + rNH_2) + 3(τNH_2) + 2(wNH_2)
3441.67	1(wCH) + 2(∂NCO + rNH_2) + 5(τNH_2)
3447.62	1(νCO + ∂CH) + 1(wCH) + 3(τNH_2)
3449.67	2(wCH) + 1(rNH_2 - νCN) + 1(τNH_2) + 1(wNH_2)
3433.10	1(νCO + ∂CH) + 3(∂NCO + rNH_2)
3436.42	2(rNH_2 - νCN) + 4(τNH_2)
3450.04	1(∂NCO + rNH_2) + 7(τNH_2) + 3(wNH_2)

Table 7: Fundamental frequencies of formamide from ref. 16. The assignments are also from ref. 16 for all modes except the NH_2 torsion and inversion.

Frequency (cm^{-1})	Assignment ν=stretch, ∂=bend, r=rock, τ=torsion, w=out-of-plane wag	
3570	$\nu_a NH_2$	asymmetric N-H_2 stretch
3448	$\nu_s NH_2$	symmetric N-H_2 stretch
2855	νCH	C-H stretch
1755	νCO + ∂CH	C=O stretch + C-H bend
1580	∂NH_2	N-H_2 bend
1390	∂CH - νCO	C-H bend - C=O stretch
1255	νCN + rNH_2 - ∂NCO	C-N stretch + N-H_2 rocking - N-C=0 bend
1090	rNH_2 - νCN	N-H_2 rocking - C-N stretch
1050	wCH	C-H out-of-plane bend
660	τNH_2	N-H_2 torsion
565	∂NCO+rNH_2	N-C=O bend + N-H_2 rocking
288.7	wNH_2	N-H_2 inversion